ENGINEERING PHYSICS AND MATHEMATICS

Analytical expression for concentration and sensitivity of a thin film semiconductor gas sensor

Kalaiselvi Selvaraj [a], **Sunil Kumar** [b], **Rajendran Lakshmanan** [a,*]

[a] *Department of Mathematics, The Madura College, Madurai 625011, Tamil Nadu, India*
[b] *Department of Mathematics, National Institute of Technology, Jamshedpur 831014, Jharkhand, India*

Abstract   In this paper, a mathematical model for gas sensing thin film semiconductor at an internal diffusion limitation for non-steady-state conditions is discussed. The model is based on diffusion equations containing a linear term related to the reaction processes. Analytical expressions for concentrations are derived using Laplace transformation. The gas sensitivity for both actual and equivalent models has been reported for all the values of reaction parameters such as rate constant and film thickness. Furthermore, in this work a complex inversion formula is employed to solve the boundary value problem. An excellent agreement with simulation data is observed. The dependence of sensitivity on temperature, film thickness and time are discussed for both actual and equivalent models.

© 2014 Production and hosting by Elsevier B.V. on behalf of Ain Shams University.
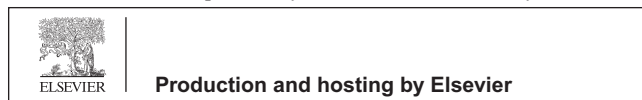
1. Introduction

Gas sensor technology has already been grown as in dispensable practice in various aspects in our life. Yet further advancements in the technology are required in order to improve sustainability of our society and quality of human life. Gas sensors play vital role in detecting, monitoring and controlling the presence of hazardous and poisonous gases in the atmosphere. It is well known fact that the gas adsorption on the surface of a semiconductor can influence its electrical conductivity [1].

Semiconductor based gas sensor can be fabricated into three types of devices, i.e., sintered block, thick film and thin film, of these sintered block and thick film devices are commercialized successfully [2]. Even though thin film devices are brought into practical use, they have remarkable characteristic features such as, fast response, low fabrication cost, ease of miniaturization, and compatibility with microelectronic circuitry [3]. Thong et al. [4] have compared gas sensor performance of SnO_2 nanowires and their hierarchical nanostructures. Every semiconductor gas sensor is provided with a porous sensing layer (resistor) of a semiconducting oxide. Under the steady-state condition, the gas concentration inside the sensing layer would decrease with increasing diffusion depth, resulting in a gas concentration profile which depends on the rates of diffusion and surface reaction [5]. Semiconductor sensors can be produced in arrays to allow sensing of

Symbol	
a	sensitivity coefficient, ppm^{-1}
a_0	pre-exponential constant, ppm^{-1}
$A = \left(\frac{3k_0}{4r}\right)^{\frac{1}{2}}\left(\frac{\pi M}{2R}\right)^{\frac{1}{4}}$	constant, nm^{-1} K$^{1/4}$
C	concentration of target gas, ppm
C_s	target gas concentration outside the film, ppm
D	diffusion coefficient, nm^2 s^{-1}
D_k	Knudsen diffusion coefficient, g/mol
E_a	apparent activation energy, kJ mol^{-1}
E_k	activation energy, kJ mol^{-1}
k	rate constant, s^{-1}
k_0	pre exponential constant, none
L	film thickness, nm
M	molecular weight, Amu
$m = L\sqrt{k/D}$	Hatta number, none
r	pore radius, nm
R	gas constant, J K^{-1} mol^{-1}
R_a	resistance of the film in air, none
R_g	resistance of the film in gas, none
S	sensitivity, none
t	time, s
u	dimensionless concentration, none
x	depth from the film surface, nm
x	distance, nm
Greek symbols	
χ	dimensionless distance, none
τ	dimensionless time, none
$\sigma(x)$	sheet conductance under exposure to the gas, none
σ_0	sheet conductance normalized in air, none

multiple species simultaneously with advances in sensitivity and detection limits which approaches parts-per-million (ppm) levels for some species. Tin oxide semiconductor gas sensors patented in 1962 by Taguchi [6]. Korotcenkov and Cho [7] analyzed the influence of film thickness of SnO_2 films deposited by a spray pyrolysis method on the operating characteristics of gas sensors. Since then stannic oxide gas sensors have undergone extensive research and development. Nowadays, Tin dioxide (SnO_2) is the most important material for use in gas sensing applications [8].

Gas sensor technology has played an important role in various fields such as in the automation of industrial processes, emission control for automobiles, and gas leakage detection in home and workplace. Specifically, the research work done on gas sensors based semiconducting metal oxides has made remarkable progress in detecting various kinds of gas molecules such as H_2, CO, hydrocarbons, NO_x, SO_x, CO_2, VOCs, and odors [9,10]. The pioneering works of Taguchi [6] in the early 1960s supported the same. Among semiconducting metal oxides, the gas sensing properties and sensing mechanism of SnO_2 have been well studied by many workers due to their excellent ability for gas sensing [11–15]. However, the understanding of working principles needs further exploration in order to develop high-performance semiconductor gas sensors required for practical applications.

Several attempts have been made to analyze/improve semiconductor gas sensors based on diffusion equations by many researchers [16–25]. Need of a sensing body with the well-defined geometry and porous structure with proper initial and boundary conditions are found to be important from the existing analysis reports [5]. Gas diffusion dynamics of a thin film semiconductor gas sensor is investigated by solving the relevant diffusion equation using the explicit finite difference method [26]. Liu et al. [27] proposed the probable application of the modified expression on explaining response of thin films to various reducing and oxidizing gases. Hosein-Babaei and Orvatinia [28] presented a mathematical model for simulation of the steady state gas sensitivity ($s = G_g/G_a$) of a thin film resistive gas sensor. Yamazoe and Shimanoe [29] discussed the gas response of oxide semiconductor film devices under control of gas diffusion and reaction effects. It is found that

no rigorous analytical expressions for the concentrations of target gas and sensitivity inside the thin film semiconductor gas sensor for all values of reaction parameters have been reported so far. Hence an attempt has been made, in this paper to come up with, approximate analytical expressions for the concentrations and sensitivity of both actual and equivalent models using Laplace transformation method. In addition the dependence of gas sensitivity on film thickness and temperature is also reported.

2. Mathematical modeling

A thin film semiconductor gas sensor is usually fabricated by depositing a porous thin layer of a semiconducting oxide on a dense substrate. The target gas molecules diffuse in the thin layer while reacting with the surface oxygen of the oxide grains. Generally, Scanning electron micrographs (SEM) demonstrate information about the surface homogeneity, surface morphology like crack free nature, pinholes, grain size, nature of the film and smoothness of the films. In optimized conditions, Metal oxide (Tin oxide thin films) illustrates a well defined and smooth uniform surface with uniform grain distribution or high crystalline nature. It provides good sensing behavior. As the layer thickness is far smaller than the layer width, the gas diffusion can be taken as one-dimensional along the direction of depth, as illustrated in Fig. 1(a) for actual
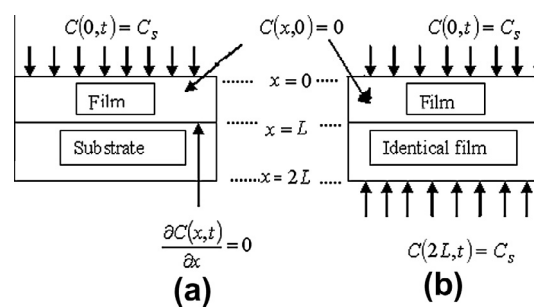

Figure 1   Modeling of thin film device: (a) for actual model (b) for equivalent model.

model and Fig. 1(b) for equivalent model . In equivalent model, the film is twice as thick as the original film, but it has no substrate to attach on, allowing the gas diffusion from both sides. For both models of the first order kinetics, diffusion equation is expressed as follows [5]:

$$\frac{\partial C(x,t)}{\partial t} = D\frac{\partial^2 C(x,t)}{\partial x^2} - kC(x,t). \tag{1}$$

Here the target gas concentration $C(x, t)$ is a function of depth from surface(x) and time (t), D is diffusion coefficient, and k is reaction constant. The initial and boundary conditions for both models (actual and equivalent) are as follows:

$$C(x,0) = \varphi(x) = 0 \tag{2a}$$

$$C(0,t) = \psi_1(t) = C_s \tag{2b}$$

The another boundary condition for the actual model is

$$\frac{\partial C}{\partial x} = \psi_2(t) = 0 \quad \text{at} \quad x = L. \tag{2c}$$

But for the equivalent model this boundary condition is replaced by

$$C(2L,t) = \psi_3(t) = C_s. \tag{2d}$$

Here suffixes 1 to 3 denote the upper and lower surfaces of the film, for both actual and equivalent models respectively. $\varphi(x)$, $\psi_1(t)$, $\psi_2(t)$ and $\psi_3(t)$ are introduced as general conditions for the convenience of mathematical treatments before they are specified to be as indicated in the later stage of derivation. Due to the symmetry of boundary conditions, the solution based on equivalent model should be also symmetric with respect to a mirror located at $x = L$. Only the upper half ($0 \leqslant x \leqslant L$) of the solution is reduced to the solution based on actual model. These models give the same solution under steady-state conditions. Under non-steady-state conditions, however, the actual model fails to give a solution of diffusion equation because the boundary conditions are not sufficient. The linear differential equation can be made dimensionless by defining the following parameters:

$$u = \frac{C}{C_s}; \quad \chi = \frac{x}{L}; \quad \tau = \frac{Dt}{L^2}; \quad m = L\sqrt{k/D}; \tag{3}$$

where u and χ represent dimensionless concentration and distance respectively. Here τ and m represent dimensionless time and Hatta number respectively. Eq. (1) can be reduced to the following dimensionless form:

$$\frac{\partial u}{\partial \tau} = \frac{\partial^2 u}{\partial \chi^2} - m^2 u. \tag{4}$$

Initial and boundary conditions (Eqs. (2a), (2b)) for both the models are reduced to

$$\tau = 0, \quad u = 0 \tag{5a}$$

$$\chi = 0, \quad u = 1 \tag{5b}$$

Another boundary condition as in Eq. (2c) for actual model can be reduced to

$$\chi = 1, \quad \frac{\partial u}{\partial \chi} = 0. \tag{5c}$$

Similarly the boundary condition Eq. (2d) for the equivalent model is reduced to

$$\chi = 2, \quad u = 1. \tag{5d}$$

3. Analytical expression of concentration profile for actual and equivalent model

The partial differential equation (4) and the boundary conditions (Eqs. (5b) and (5c)) in Laplace space becomes as follows:

$$\frac{d^2\bar{u}}{d\chi^2} = (s + m^2)\bar{u}. \tag{6}$$

where $\bar{u}$ denotes the Laplace transform of a function $\boldsymbol{u}$. Now, the boundary conditions for actual model becomes,

$$\chi = 0, \quad \bar{u} = \frac{1}{s} \tag{7a}$$

$$\chi = 1, \frac{\partial \bar{u}}{\partial \chi} = 0. \tag{7b}$$

The analytical solution for Eq. (6) (Appendix A) is

$$u(\chi,\tau) = \frac{\cosh((1-\chi)m)}{\cosh(m)}$$
$$- \sum_{n=1}^{\infty} \frac{(-1)^{-n}(2n+1)\pi \exp\left[-\left(m^2 + \frac{(2n+1)^2\pi^2}{4}\right)\tau\right]\cos\left(\left(\frac{(2n+1)\pi}{2}\right)(1-\chi)\right)}{\left(m^2 + \frac{(2n+1)^2\pi^2}{4}\right)}. \tag{8}$$

Now, the boundary conditions for equivalent model become,

$$\chi = 0, \quad \bar{u} = \frac{1}{s} \tag{9a}$$

$$\chi = 2, \quad \bar{u} = \frac{1}{s} \tag{9b}$$

Similarly the analytical solution of Eq. (6) for equivalent model is as follows:

$$u(\chi,\tau) = \frac{\sinh(m\chi) - \sinh[m(\chi-2)]}{\sinh(2m)}$$
$$- \sum_{n=1}^{\infty} \frac{(-1)^{-n}n\pi\left[\sin\frac{n\pi}{2}(\chi-2) - \sin\left(\frac{n\pi}{2}\chi\right)\right]\exp\left[-\left(\frac{n^2\pi^2}{4} + m^2\right)\tau\right]}{2\left(\frac{n^2\pi^2}{4} + m^2\right)}. \tag{10}$$

4. Analytical expression of sensitivity for actual model

Let us consider that the thin film is a uniform stack of infinitesimally thin sheets, the electric conductance of each of which is given by $\sigma(x)$, where x is depth from the film surface. The conductance of the whole film is then derived by integrating $\sigma(x)$ over the whole range of x (x = 0 − L). Also we can assume that [5].

$$\sigma(\text{x}) = \sigma_0(1 + aC). \tag{11}$$

Here a is sensitivity coefficient and σ_0 is conductance in air. The resistance in air (R_a) and resistance in the air containing target gas (R_g) can be expressed as follows:

$$\frac{1}{R_a} = \int_0^1 \sigma_0 d\chi, \quad \frac{1}{R_g} = \int_0^1 \sigma_x d\chi. \tag{12}$$

Gas sensitivity (s) is defined as the ratio of resistance in air (R_a) to resistance in the air containing target gas (R_g). This can be obtained using Eq. (12) as follows:

$$s(m,\tau) = \frac{R_a}{R_g} = \frac{\int_0^1 \sigma_x d\chi}{\int_0^1 \sigma_0 d\chi} = 1 + a\int_0^1 C(\chi,\tau)d\chi$$

$$= 1 + a\left[\frac{\tanh(m)}{m} + \frac{\sum_{n=1}^{\infty} 2(2n+1)\pi e^{-\left(m^2 + \frac{(2n+1)^2\pi^2}{4}\right)\tau}}{\left(m^2 + \frac{(2n+1)^2\pi^2}{4}\right)}\right].$$

$$(13)$$

5. Analytical expression of sensitivity for equivalent model

For equivalent model the resistance in air (R_a) and resistance in the air containing target gas (R_g) can be expressed in the following form:

$$\frac{1}{R_a} = \int_0^2 \sigma_0 d\chi, \quad \frac{1}{R_g} = \int_0^2 \sigma_X d\chi \qquad (14)$$

Using Eq. (14), the analytical expression of sensitivity for equivalent model is obtained as,

$$s(m,\tau) = \frac{R_a}{R_g} = \frac{\int_0^2 \sigma_x d\chi}{\int_0^2 \sigma_0 d\chi} = 1 + a\int_0^2 C(\chi,\tau)d\chi$$

$$= 1 + a\left[\frac{2}{m}\left[\frac{1}{\tanh(2m)} - \frac{1}{\sinh(2m)}\right]\right.$$

$$\left. -2\sum_{n=1}^{\infty}(-1+(-1)^n)\frac{\exp\left(-\left(m^2 + \frac{n^2\pi^2}{4}\right)\right)\tau}{\left(m^2 + \frac{n^2\pi^2}{4}\right)}\right] \qquad (15)$$

6. Analytical expression of sensitivity on operating temperature for actual and equivalent models

The dependence of sensitivity on temperature is considered here. It is obvious that Knudsen diffusion coefficient D_k, the rate constant k and sensitivity coefficient a can be represented in terms of temperature as follows:

$$D_k = \frac{4r}{3}\sqrt{\frac{2RT}{\pi M}} \qquad (16)$$

$$k = k_0 \exp\left(-\frac{E_k}{RT}\right) \qquad (17)$$

$$a = a_0 \exp\left(-\frac{E_a}{RT}\right) \qquad (18)$$

Combining Eqs. (16)–(18) with Eq. (13), the following analytical expression of sensitivity for actual model can be obtained as,

$$s(m,\tau) = 1 + a_0 \exp\left(-\frac{E_a}{RT}\right)$$

$$\left[\frac{\tanh(m)}{m} + \frac{\sum_{n=1}^{\infty} 2(2n+1)\pi \exp\left(-\left(m^2 + \frac{(2n+1)^2\pi^2}{4}\right)\tau\right)}{\left(m^2 + \frac{(2n+1)^2\pi^2}{4}\right)}\right]$$

$$(19)$$

where $m = ALT^{-0.25} \exp(-E_k/2RT)$. By combining Eqs. (16)–(18) with Eq. (13), followed by rearranging, the analytical expression of sensitivity for equivalent model can be obtained as,

$$s(m,\tau) = 1 + a_0 \exp\left(-\frac{E_a}{RT}\right)\left[\frac{2}{m}\left[\frac{1}{\tanh(2m)} - \frac{1}{\sinh(2m)}\right]\right.$$

$$\left. -2\sum_{n=1}^{\infty}(-1+(-1)^n)\frac{\exp\left(-(m^2 + \frac{n^2\pi^2}{4})\right)\tau}{\left(m^2 + \frac{n^2\pi^2}{4}\right)}\right]. \qquad (20)$$

7. Numerical simulation

The diffusion equation (Eq. (6)) for the boundary conditions (Eqs. (7a), (7b), (9a), (9b)) are solved by numerical methods. The function pdex4 in Matlab software, which is a function of solving the initial boundary value problems for partial differential equations, is used to solve these equations. Numerical solution obtained from this function is compared with the analytical results which are depicted in Fig. 2. An excellent agreement for all values of time τ is observed. The corresponding Matlab program is made available in Appendix B.
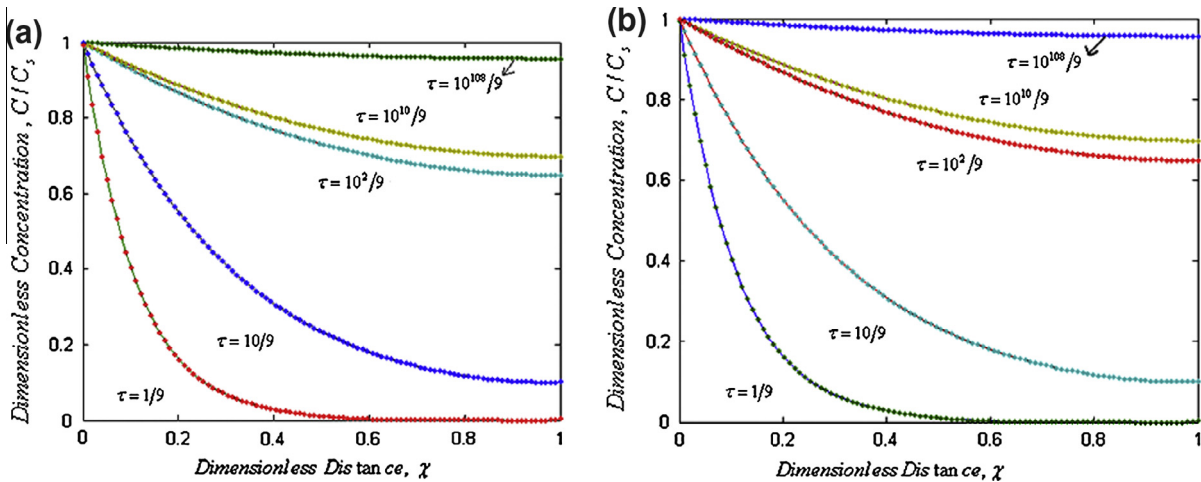

Figure 2 Dimensionless concentration versus the dimensionless distance for various values of τ and for the fixed value of $m(=9)$, $L = 300$ nm, $D = 10^{12}$ nm^2 s^{-1}, $k = 9 * 10^8$ s^{-1}. (–) represents analytical results and (…) represents numerical results. (a) For actual model (Eq. (8)); (b) for equivalent model (Eq. (10)).
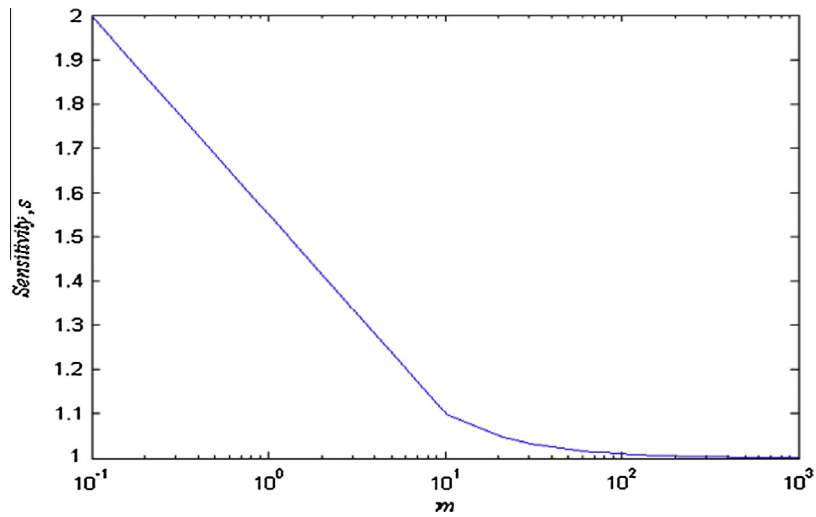
Figure 3 Generalized expression of the gas sensitivity of thin films versus non-dimensional parameter, $(m(= L\sqrt{k/D}))$ for actual model using Eq. (13) at $\tau = 1$.
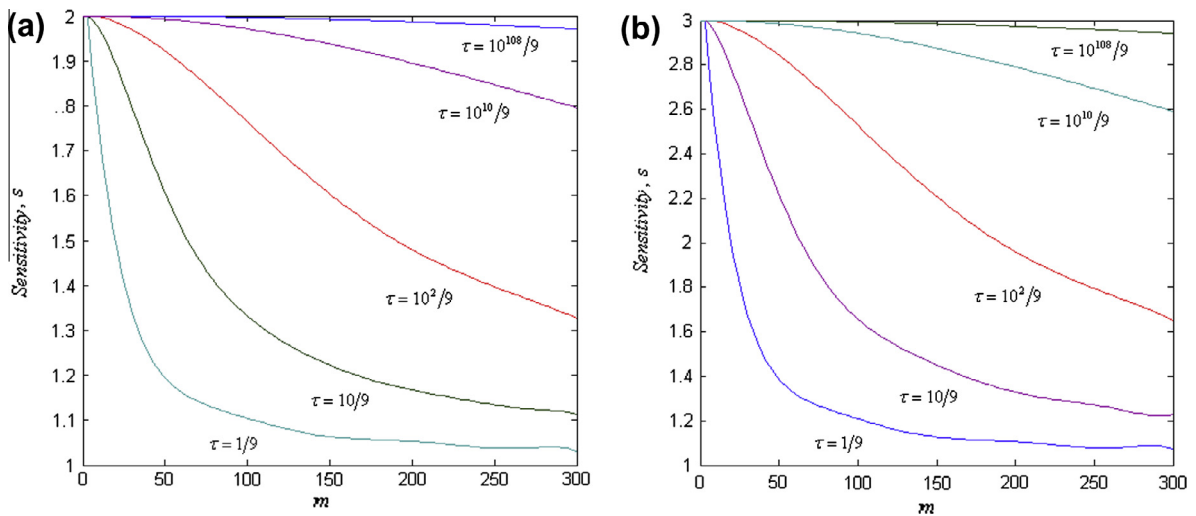

Figure 4 Non-steady state gas sensitivity versus m at various periods of time τ. (a) for actual model (Eq. (13)); (b) for equivalent model (Eq. (15)).
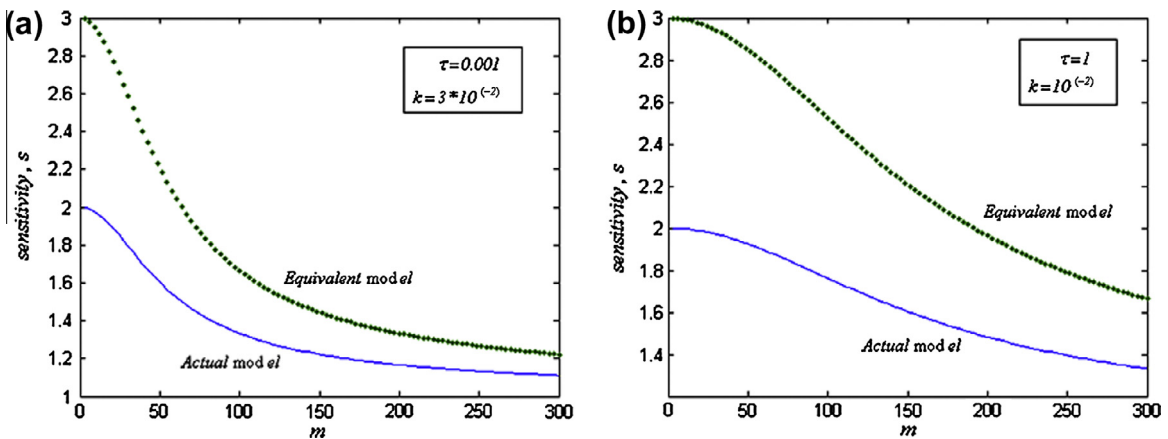

Figure 5 Non-steady state gas sensitivity versus m. (a) for actual model (Eq. (13)); (b) for equivalent model (Eq. (15)).
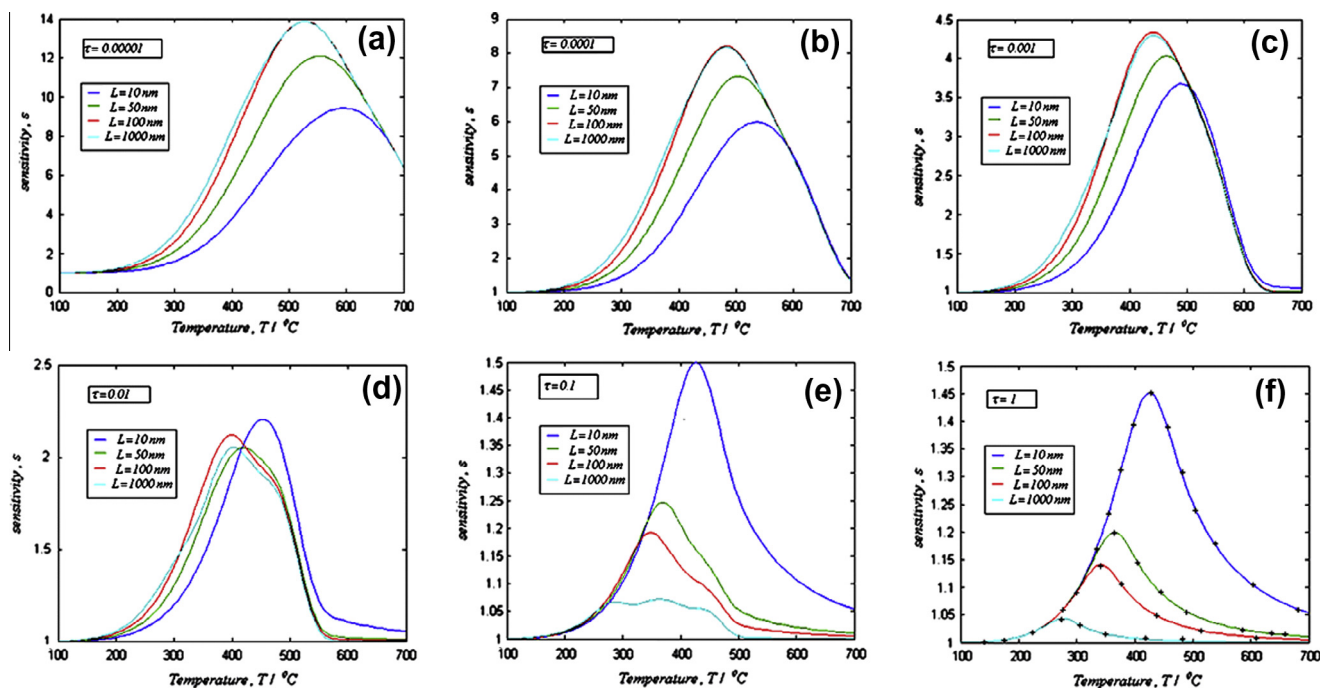
Figure 6 Actual model non-steady state gas sensitivity versus temperature for various values of film thickness, L and time, τ simulated under the conditions for $E_a = 50 \text{ kJ mol}^{-1}$, $E_k = 200 \text{ kJ mol}^{-1}$, $A = 1.7 * 10^7 \text{ nm}^{-1} \text{ K}^{1/4}$, $a_0 = 3400 \text{ ppm}^{-1}$ (Eq. (19)). Solid line denotes the non-steady state sensitivity. In (f) '+' denotes the steady state sensitivity.

Figure 7 Equivalent model non-steady state gas sensitivity versus temperature for various values of film thickness, L and time, τ simulated under the conditions for $E_a = 50 \text{ kJ mol}^{-1}$, $E_k = 200 \text{ kJ mol}^{-1}$, $A = 1.7 * 10^7 \text{ nm}^{-1} \text{ K}^{1/4}$, $a_0 = 3400 \text{ ppm}^{-1}$ (Eq. (20)). Solid line denotes the non-steady state sensitivity. In (f) '+' denotes the steady state sensitivity.
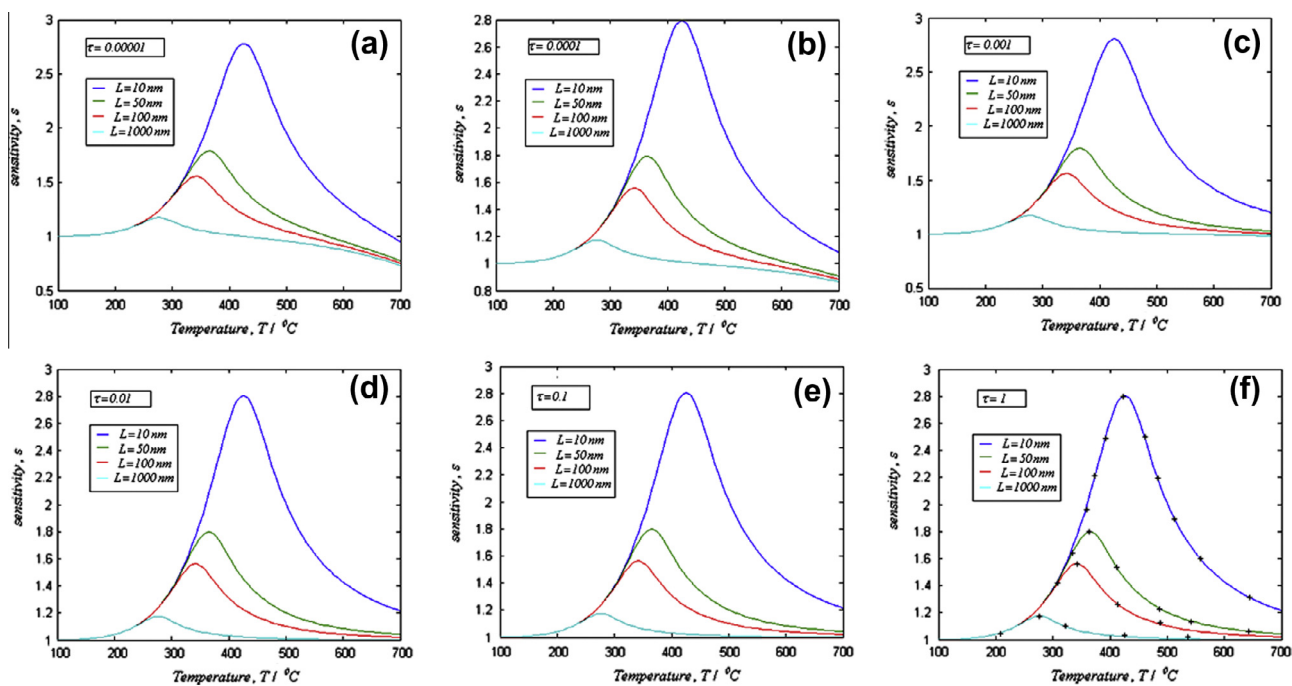
8. Results and discussion

Eqs. (8) and (10) are the new and simple approximate analytical expressions for the gas concentration profile calculated using Laplace transformation method. The analytical expressions of concentration $u(\chi, \tau)$ for various values of dimensionless reaction parameter m and dimensionless time τ are compared with numerical solution.

Fig. 2(a) and (b) shows the variation in dimensionless concentration versus the dimensionless distance for various values of time τ and for some fixed value of $m(= 9)$. Obviously the profile changes sharply with changing time τ. From this figure, it also observed that the concentration profile of gas decreases gradually when τ decreases and the value of the concentration is uniform when $\tau \geqslant 10^{108}/9$ in both models.

Fig. 3 shows the generalized expression of the gas sensitivity of thin film at a fixed temperature in terms of non-dimensional parameter, m. Fig. 4(a) and (b) shows the sensitivity versus m using Eqs. (13)–(15) for various values of τ for both actual and equivalent models.

From Fig. 5 it is inferred that the sensitivity of equivalent model is always greater than actual model. Also sensitivity for both model decreases when m increases. Non-steady state gas sensitivity versus temperature for various values of film thickness, L, temperature, T and time τ is plotted in Fig. 6 (actual model) and Fig. 7 (equivalent model). From these figures it is inferred that sensitivity reaches the maximum value when $400\,°C \leqslant T \leqslant 500\,°c$. For actual model this maximum value decreases when time increases, whereas the maximum value is constant for equivalent model. Also in both models, sensitivity reaches the steady state value (or constant value) when $\tau = 1$ (Figs. 6(f) and 7(f)). Sensitivity always decreases when film thickness, L increases.

9. Conclusion

The time dependent reaction–diffusion equations in semiconductor gas sensor have been solved analytically and numerically. In the present study, analytical expression corresponding to the concentration profile in semiconductor gas sensor for actual and equivalent model in terms of all reaction parameter, (m) is presented. It is observed that the results obtained using the analytical expression show a good conformity with numerical simulation results. The dependency of gas sensitivity on film thickness and temperature for various values of time for both actual and equivalent models are also discussed.

Appendix A. Solutions of Eq. (4) using complex inversion formula

The solution of Eq. (6) for the boundary condition Eqs. (7a), (7b) is

$$\bar{u}(\chi, \tau) = \frac{\cosh[(1 - \chi)\sqrt{s + m^2}]}{s \cosh\left(\sqrt{s + m^2}\right)} \tag{A1}$$

We can find the inverse Laplace transform for the above Eq. (A1) using complex inversion formula. If $\bar{y}(s)$ represents the Laplace transform of a function $y(\tau)$, then according to the complex inversion formula we can state that

$$y(\tau) = \frac{1}{2\pi i} \int_{c-i\infty}^{c+i\infty} \exp[s\tau]\bar{y}(s)ds = \frac{1}{2\pi i} \oint_c \exp[s\tau]\bar{y}(s)ds \tag{A2}$$

where the integration in Eq. (A2) is to be performed along a line $s = c$ in the complex plane where $s = x + iy$. The real number c is chosen such that $s = c$ lies to the right of all the singularities, but is otherwise assumed to be arbitrary. In practice, the integral is evaluated by considering the contour integral presented on the r.h.s of Eq. (A1), which is evaluated using the so-called Bromwich contour. The contour integral is then evaluated using the residue theorem which states for any analytic function $F(z)$

$$\oint_c F(z)dz = 2\pi i \sum_n \text{Res}[F(z)]_{z=z_n} \tag{A3}$$

Where the residues are computed at the poles of the function $F(z)$. Hence from Eq. (A3) we note that:

$$y(\tau) = \sum_n \text{Res}[\exp[s\tau]\bar{y}(s)]_{s=s_n} \tag{A4}$$

From the theory of complex variables we can show that the residue of a function $F(z)$ at a simple pole at $z = a$ is given by:

$$\text{Res}[F(z)]_{z=a} = \lim_{z \to a}\{(z - a)F(z)\} \tag{A5}$$

Hence in order to invert Eq. (4), we need to evaluate $\text{Res}\left[\cosh(1 - \chi)\left(\sqrt{s + m^2}\right)/s\cosh\left(\sqrt{s + m^2}\right)\right]$. Now the poles are obtained from $s\cosh\left(\sqrt{s + m^2}\right) = 0$. Hence there is a simple pole at $s = 0$ and there are infinitely many poles given by the solution of the equation $\cosh\left(\sqrt{s + m^2}\right) = 0$ and so $s_n = -\left[\frac{(2n+1)^2\pi^2}{4} + m^2\right]$ with $n = 1, 2, \ldots$. Hence we note that:

$$S(\chi, \tau) = \text{Res}\left[\frac{\cosh(1 - \chi)\left(\sqrt{s + m^2}\right)}{s\cosh\left(\sqrt{s + m^2}\right)}\right]_{s=0}$$
$$+ \text{Res}\left[\frac{\cosh(1 - \chi)\left(\sqrt{s + m^2}\right)}{s\cosh\left(\sqrt{s + m^2}\right)}\right]_{s=s_n}$$
$$= \lim_{s \to 0}(s - 0)\left\{\exp(s\tau)\frac{\cosh(1 - \chi)\left(\sqrt{s + m^2}\right)}{s\cosh\left(\sqrt{s + m^2}\right)}\right\}$$
$$+ \lim_{s \to s_n}(s$$
$$- s_n)\left\{\exp(s\tau)\frac{\cosh(1 - \chi)\left(\sqrt{s + m^2}\right)}{s\cosh\left(\sqrt{s + m^2}\right)}\right\} \tag{A6}$$

The first residue in Eq. (A6) is given by

$$\text{Res}\left[\frac{\cosh(1-\chi)\left(\sqrt{s+m^2}\right)}{s\cosh\left(\sqrt{s+m^2}\right)}\right]_{s=0}$$

$$= \lim_{s\to 0}\left\{\exp(s\tau)\frac{\cosh(1-\chi)\left(\sqrt{s+m^2}\right)}{s\cosh\left(\sqrt{s+m^2}\right)}\right\}$$

$$= \frac{\cosh[(1-\chi)m]}{\cosh(m)} \tag{A7}$$

The second residue in Eq. (A6) can be evaluated as follows. It is established that if $F(z)$ can be expressed as $F(z) = f(z)/g(z)$, where the functions f and g are analytic at $s = s_n$ and $g(s_n) = 0$ while $g'(s_n) \neq 0$ and $f(s_n) \neq 0$. Then, $\text{Res}[F(z)]_{s=s_n} = \sum_{n=0}^{\infty}\frac{f(s_n)}{g'(s_n)}\exp[s_n\tau]$. Hence we can show that:

$$\lim_{s\to s_n} e^{s\tau}\frac{\cosh(1-\chi)\left(\sqrt{s+m^2}\right)}{s\frac{d}{ds}\cosh(\sqrt{s+m^2})}$$

$$= \lim_{s\to s_n} e^{st}\frac{\cosh(1-\chi)\left(\sqrt{s+m^2}\right)(2\sqrt{s+m^2})}{s_n\sinh\left(\sqrt{s+m^2}\right)}$$

$$= \frac{2\exp\left[-\left\{\frac{(2n+1)^2\pi^2}{4}+m^2\right\}\tau\right]\cosh\left[\frac{i(2n+1)\pi}{2}(1-\chi)\right]\sqrt{s+m^2}}{-\left(\frac{(2n+1)^2\pi^2}{4}+m^2\right)\sinh\left(\frac{i(2n+1)\pi}{2}\right)},$$

$$n = 1, 2 \ldots . \tag{A8}$$

Using $\cosh(i\theta) = \cos(\theta)$ and $\sinh(i\theta) = i\sin(\theta)$ the above results becomes

$$\lim_{s\to s_n} e^{st}\frac{\cosh(1-\chi)\left(\sqrt{s+m^2}\right)}{s\cosh\left(\sqrt{s+m^2}\right)} =$$

$$-\sum_{n=1}^{\infty}\frac{(-1)^{-n}(2n+1)\pi\exp\left[-\left(\frac{(2n+1)^2\pi^2}{4}+m^2\right)\tau\right]\cos\left[\left(\frac{(2n+1)}{2}\right)(1-\chi)\right]}{\left(\frac{(2n+1)^2\pi^2}{4}+m^2\right)} \tag{A9}$$

Adding Eqs. (A7) and (A9) we obtain Eq. (8) in the text.

Appendix B. The Matlab program to find the numerical solution of Eq. (8)

```
function pdex1
m = 0;
x = linspace(0,1);
t = linspace(0, (1/9));
sol = pdepe(m,@pdex1pde,@pdex1ic,@pdex1bc,x,t);
u1 = sol(:,:,1);
figure
plot(x,u1(end,:))
title('u1(x,t)')
function [c,f,s] = pdex1pde(x,t,u,DuDx)
m1 = 300 * 3 * 10^(−2);
c = 1;
f = 1. * DuDx;
F = −m1^2 * u(1);
s = F;
function u0 = pdex1ic(x);
u0 = 0;
function [pl,ql,pr,qr] = pdex1bc(xl,ul,xr,ur,t)
pl = ul(1) − 1;
ql = 0;
pr = 0;
qr = 1;
```

References

[1] Makhija KK, Arabindaray, Patel RM, Trivedi UB, Kapse HN. Indium oxide thin film based ammonia gas and ethanol vapour sensor. Indian Academy of Sciences Bull Mater Sci 2005;28(1):9–17.

[2] Baik NS, Sakai G, Miura N, Yamazoe N. Hydrothermally treated sol solution of tin oxide for thin-film gas sensor. Sens Actuators B 2000;63:74–9.

[3] Brown JR, Cheney MT, Haycock PW, Houlton DJ, Jones AC, Williams EW. The gas-sensing properties of tin oxide thin films deposited by metallorganic chemical vapor deposition. J Electrochem Soc 1997;144:295–9.

[4] Thong Le Viet, Loan Le Thi Ngoc, Van Hieu Nguyen. Comparative study of gas sensor performance of Sno_2 nano wires and their hierarchical nanostructures. Sens Actuators B 2010;150:112–9.

[5] Sakai Go, Matsunaga Naoki, Kengoshimanoe, Yamazoe Noboru. Theory of gas diffusion controlled sensitivity for thin film semiconductor gas sensor. Sens Actuators B 2001;80:125–31.

[6] Taguchi N. Patent 45-38200; 1962.

[7] Korotcenkov G, Cho BK. Thin film SnO_2 – based gas sensors: film thickness influence. Sens Actuators B 2009;142:321–30.

[8] Miller TA, Bakrania SD, Perez C, Wooldridge MS. Nano structured Tin dioxide materials for gas sensor applications Michigan 48109-2125, USA [chapter 30].

[9] Yamazoe N. Toward innovations of gas sensor technology. Sens Actuators B: Chem 2005;108:2–14.

[10] Yamazoe N, Sakai G, Shimanoe K. Oxide semiconductor gas sensors. Catal Surv Asia 2003;1:63–75.

[11] Weimar U, Schierbaum KD, Göpel W, Kowalkowski R. Pattern recognition methods for gas mixture analysis: application to sensor arrays based upon SnO_2. Sens Actuators B: Chem 1990;1:93–6.

[12] Bârsan N, Ionescu R. The mechanism of the interaction between CO and a SnO_2 surface: the role of water vapour. Sens Actuators B: Chem 1993;12:71–5.

[13] Weimar U, Göpel W. A.c. measurements on tin oxide sensors to improve selectivities and sensitivities. Sens Actuators B: Chem 1995;26:13–8.

[14] Göpel W, Schierbaum KD. SnO_2 sensors: current status and future prospects. Sens Actuators B: Chem 1995;26:1–12.

[15] Kappler J, Bârsan N, Weimar U, Dièguez A, Alay JL, Romano-Rodriguez A, Morante JR, Göpel W. Correlation between XPS, Raman and TEM measurements and the gas sensitivity of Pt and Pd doped SnO_2-based gas sensors. Fresen J Anal Chem 1998;361:110–4.

[16] Williams DE, Pratt KFE. Theory of self-diagnostic sensor array devices using gas-sensitive resistors. J Chem Soc, Faraday Trans 1995;91(13):1961–6.

[17] Gardner JW. A diffusion–reaction model of electrical conduction in tin oxide gas sensors. Semicond Sci Technol 1989;4:345–50.

[18] Gardner JW. Electrical conduction in solid-states gas sensors. Sens Actuators 1989;18:373–87.

[19] Gardner JW. A non-linear diffusion–reaction model of electrical conduction in semiconductor gas sensors. Sens Actuators B 1990;1:166–70.

[20] Gardner JW. Effect of electrode geometry on gas sensitivity of lead phthalocyanine thin films. Sens Actuators B 1992;9:133–42.

[21] Vilanova X, Llobet E, Alcubilla R, Sueiras JE, Correig X. Analysis of the conductance transient in thick-film thin oxide gas sensors. Sens Actuators B 1996;31:175–80.

[22] Llobet E, Vilanova X, Brezmes J, Sueiras JE, Alcubilla R, Correig X. Steady-state and transient behavior of thick-film tin oxide sensors in the presence of gas mixtures. J Electrochem Soc 1998;145(5):1772–9.

[23] Ju YH, Hsieh C, Liu CJ. The surface reaction and diffusion of NO_2 in lead phthalocyanine thin film. Thin Solid Films 1999;342:238–43.

[24] Lu H, Ma W, Gao J, Li J. Diffusion–reaction theory for conductance response in metal oxide gas sensing films. Sens Actuators B 2000;66:228–31.

[25] Matsunaga Naoki, sakai Go, Kengoshimanoe, Yamazoe Noboru. Formulation of gas diffusion dynamics for thin film semiconductor gas sensor based on simple reaction–diffusion equation. Sens Actuators B 2003;96:226–33.

[26] Savović Svetislav, Djordjevich Alexandar. Finite difference solution of the diffusion equation describing the response and recovery of thin film semiconductor gas sensors. Sens Actuators B 2012;166–167:200–4.

[27] Liu Jianqiao, Gong Shuping, Xia Jing, Quan Lin, Liu Huan, Zhou Dongxiang. The sensor response of tin oxide thin films to different gas concentration and the modification of the gas diffusion theory. Sens Actuators B 2009;138:289–95.

[28] Hosein-Babaei Faramarz, Orvatinia Mohammad. Analysis of thickness dependence of the sensitivity in thin film resistive gas sensors. Sens Actuators B 2003;89:256–61.

[29] Yamazoe Noboru, Shimanoe Kengo. Theoretical approach to the gas response of oxide semiconductor film devices under control of gas diffusion and reaction effects. Sens Actuators B 2011;154:277–82.

Dr. L. Rajendran received his M.Sc. in Mathematics in 1981 from Presidency College, Chennai, TN, India. He obtained his Ph.D. in Applied Mathematics from Alagappa University, Karaikudi, TN, India during 2000. At present, he is an Assistant Professor in Mathematics at Madura College, Madurai, TN, India. Before this position (1986–2007), he was working as a Post Graduate Assistant in Mathematics at SMSV Higher Secondary School, Karaikudi, TN, India. He has 20 years teaching experience and 15 years research experience. He has authored and coauthor over 110 research publications including about 40 scholarly articles in peer-reviewed journals. He visited institute fur Organische Chemie, University at Tubingen, D-72076 Tubingen, Germany in year 2003 under INSA and DFG Post-doctoral Research Fellowship. He also visited polish academic of science, Poland in 2011. Currently he have three research projects from DST, CSIR and UGC. His current research interests include mathematical and computational modeling of electrochemical biosensor.

S. Kalaiselvi received her M.Sc. in Mathematics from Madurai Kamaraj University, Madurai, TamilNadu, India during 1999. She has received her M. Phil., (2001) in Mathematics from Madurai Kamaraj University, Madurai, Tamil Nadu, India. Also she is doing her Ph. D. in ''Mathematical modeling and non-linear reaction diffusion equations for boundary value problems'' at Madurai Kamaraj University, Madurai, Tamil Nadu, India under the guidance of Dr. L. Rajendran. She has 4 years of teaching experience and 1 year research experience. Her present research interest includes: Mathematical modeling based on differential equations and asymptotic approximations, analysis of non-linear reaction diffusion processes in gas sensors.

Dr. Sunil Kumar is an Assistant Professor in the Department of Mathematics, National Institute of Technology, Jamshedpur, 831014, Jharkhand, India. He received his M.Phil., from CSJM University, Kanpur, and Ph.D. degree from the Indian Institute of Technology, BHU, Varanasi in 2012. He is editor of fourteen international journals. His current research mainly covers fractional calculus, Homotopy methods, Wavelet methods, analytical and numerical solutions of nonlinear problems arising in applied sciences and engineering phenomena.